===== **SEMICONDUCTORS** =====

Electronic Structure of $CuCl_{1-x}Br_x$ Solid Solutions: First-Principles Calculations in the meta-GGA Approximation

A. V. Kosobutsky[a, b],* and A. B. Gordienko[b]

[a] *National Research Tomsk State University, pr. Lenina 36, Tomsk, 634050 Russia*
[b] *Kemerovo State University, ul. Krasnaya 6, Kemerovo, 650043 Russia*
* *e-mail: kosobutsky@kemsu.ru*
Received April 16, 2015

Abstract—The electronic structure of CuCl and CuBr compounds and their solid solutions $CuCl_{1-x}Br_x$ ($x = 0.25, 0.50, 0.75$) has been calculated in the framework of the density functional theory. The calculations have been performed in the basis of pseudoatomic orbitals using the simple local approximation (LDA) and the new meta-GGA exchange potential TB09, which, to a large extent, compensates the LDA error in the description of the position of conduction bands in semiconductors. A comparative analysis of the main characteristics of the electronic structure of binary compounds and their solutions has been carried out. It has been found that the composition dependence of the band gap $E_g(x)$ has a small downward bowing with the coefficient $b \sim 0.09$ eV.

1. INTRODUCTION

Copper halides (CuCl, CuBr, CuI) are promising materials for use in catalysis, preparation of transparent conductive coatings, composite nanomaterials with new properties, and electronic devices [1—4]. According to their characteristics, these materials belong to the class of direct-band-gap semiconductors with the band gap $E_g \sim 3$ eV. The highest value of the band gap in this group of compounds is observed in copper chloride CuCl with $E_g = 3.39$ eV at room temperature, which is comparable to the values of E_g for optoelectronic materials, such as gallium nitride and zinc oxide. The lattice constant of CuCl is rather close to that of silicon, which allows the effective use of silicon substrates for growing thin-film layers of copper chloride [4].

In recent years, the increased interest in electronic properties of copper halides [1, 2, 4, 5] poses the problem of an adequate theoretical description of their electronic structure with the use of modern methods of first-principles calculations. The most attention was paid in the past to binary semiconductors. In particular, first-principles calculations of the band structure and optical functions of CuCl and CuBr under normal conditions and at a pressure were performed in [6—8] within the framework of the density functional theory (DFT) using the full-potential linearized augmented plane wave (FP-LAPW) method. The performed theoretical studies made it possible to estimate the lattice constants, binding energies, elastic and dielectric characteristics, bulk moduli, and parameters of the most important interband transitions. The FP-LAPW and first-principles pseudopotential approximations

were also used in [9, 10] for the study of $CuCl_{1-x}Br_x$ solid solutions. It should be noted that FP-LAPW represents one of the most accurate methods for calculating structural and electronic properties of solids. However, the results of DFT computations of the interband transitions and related characteristics depend substantially on the choice of the approximation for taking into account the exchange-correlation effects. Earlier studies were performed predominantly using the local density approximation (LDA) or generalized gradient approximation (GGA), which are highly effective in calculations of lattice parameters and binding energies. At the same time, the well-known disadvantage of LDA/GGA is a significant underestimation of the band gap E_g of dielectrics and semiconductors. In particular, the estimations made in [8—10] gave the band gaps of CuCl and CuBr in the range of 0.4—0.5 eV, which accounts for only ~15% of the corresponding experimental values.

According to the classification of exchange-correlation functionals in line with their level of complexity, which was proposed by Perdew et al. [11], the approximations LDA and GGA occupy the first and second rungs of the hierarchy ladder, respectively. The complication of the GGA functionals as compared to the LDA ones consists in using information on the electron density gradient, which has increased the accuracy of total-energy calculations and provided, since the 1990s, the wide use of the DFT method for solving problems in quantum chemistry. The third rung is occupied by the meta-GGA functionals, which, apart from the electron density and its gradient, explicitly depend on the kinetic energy density. Examples are

TPSS [11], M06-L [12], and TB09 [13], which are being actively discussed in the literature.

The purpose of this work is to investigate the electronic structure of CuCl$_{1-x}$Br$_x$ by employing the TB09 potential recently proposed by Tran and Blaha (mBJLDA) [13], which can increase the accuracy of E_g calculations for solids within DFT.

2. THEORY AND CALCULATION METHOD

The work of Tran and Blaha [13] is based on the success of the optimized effective potential (OEP) method in reproducing the values of E_g and is the development of the studies performed by Becke and Johnson [14], who made an attempt to approximate the exact OEP exchange potential by an expression depending only on the total electron density and the kinetic energy density for occupied states. The Becke−Johnson exchange potential (υ_x^{BJ}), being semilocal in its design, adequately reproduces the OEP step structure and derivative discontinuity with respect to the number of particles. In [13], the modification of the potential υ_x^{BJ} was proposed in the form

$$\upsilon_x^{TB09}(\mathbf{r}) = c\upsilon_x^{BR}(\mathbf{r}) + (3c-2)\frac{1}{\pi}\sqrt{\frac{5}{12}}\sqrt{\frac{2t(\mathbf{r})}{\rho(\mathbf{r})}}, \quad (1)$$

where $\upsilon_x^{BR}(\mathbf{r})$ is the Becke−Roussel potential [15]; $\rho(\mathbf{r})$ is the electron density; $t(\mathbf{r}) = (1/2)\sum_i \nabla\psi_i^* \times \nabla\psi_i$ is the kinetic energy density of the electronic subsystem; and c is a free parameter, for which the following analytical expression was given in [13]:

$$c = \alpha + \beta\left(\frac{1}{V_c}\int_{V_c}|\nabla\rho(\mathbf{r})|\rho^{-1}(\mathbf{r})d\mathbf{r}\right)^{1/2}. \quad (2)$$

The integration in expression (2) is performed over the unit cell volume V_c, and the parameters α and β are determined by minimizing the mean absolute relative error of the band gap E_g for the group of semiconductors and dielectrics.

The correlation effects in the calculations with the TB09 potential are described within the LDA approach. In general, this calculation scheme is comparable in computational expense to the standard GGA forms, but substantially exceeds GGA in the accuracy of the evaluation of the band gap E_g, and, in some cases, approaches quasiparticle methods, such as the GW approximation [16, 17].

In this work, the electronic structure of binary copper halides and their solutions was calculated using ab initio separable pseudopotentials [18] and the basis of localized atomic pseudo-orbitals (PAO) [19] given in a numerical form. In order to calculate all types of multicenter integrals, the Bloch functions constructed from PAO (Cu(sd), Cl(spd), Br(spd)) were expanded in plane waves with energies up to 169 Ry. The electron density and the kinetic energy density were calculated by the special-point method on a $4 \times 4 \times 4$ k-point mesh. The described approach was successfully employed earlier in the study of the CuBS$_2$ crystal [20]. The calculations of the electronic properties in the PAO basis were performed for optimized crystal structures. The CuCl$_{1-x}$Br$_x$ solid solution was simulated by a $2 \times 2 \times 2$ supercell containing 16 atoms. The structure was optimized using the Quantum ESPRESSO package [21] within the LDA approach with the projector augmented wave method and calculation parameters providing a sufficiently high level of convergence of the structural parameters.

3. RESULTS AND DISCUSSION

The CuCl and CuBr compounds crystallize in the sphalerite structure with the lattice parameters of 5.409 and 5.677 Å at $T \sim 20$ K, respectively [22]. The corresponding theoretical values obtained in our work are equal to 5.219 and 5.525 Å, respectively. The calculated lattice parameters, as expected, are less than the experimental values due to the use of the local density approximation at the stage of optimization of the structure. It should be noted that the lattice parameters obtained for CuCl and CuBr are very close to the results of the full-potential calculations [16] in the framework of the LDA (5.210 and 5.526 Å, respectively).

In earlier studies, the main method used for the simulation of CuCl$_{1-x}$Br$_x$, CuCl$_{1-x}$I$_x$, and CuBr$_{1-x}$I$_x$ solid solutions was the virtual crystal approximation (VCA) [9, 23]. Apparently, the only exception is the work by El Haj Hassan and Zaoui [10], who considered an eight-atom cubic cell for CuCl$_{0.5}$Br$_{0.5}$. A principal advantage of the VCA is the possibility of studying mixed crystals by employing the unit cell of the initial material, i.e., without complication of the crystal structure. This approach is characterized by the simplicity of implementation and low computational costs and makes it possible to analyze the characteristics of a solid solution as continuous functions of the impurity concentration. However, VCA does not allow one to take into account local distortions of the crystal structure and fluctuations of the composition, which, in many aspects, determine the physical properties of mixed crystals. For this reason, in our work, the CuCl$_{1-x}$Br$_x$ solid solutions were considered using the supercell method. Direct calculations were performed for $2 \times 2 \times 2$ supercells with the bromine concentrations $x = 0.25$, 0.50, and 0.75. The optimized lattice parameters with respect to the sphalerite unit cell are presented in Fig. 1, where for convenience the calculated values for CuCl and CuBr are connected by a straight line. It can be seen that the theoretical data fit well into the straight line (Vegard's law), which is in
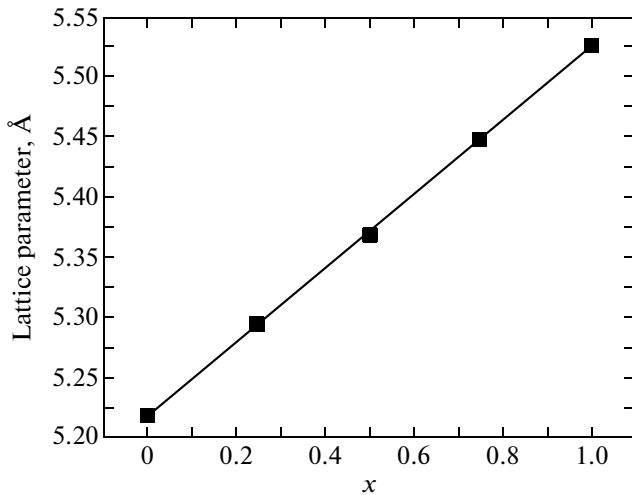
Fig. 1. Lattice parameter of the mixed $CuCl_{1-x}Br_x$ crystal as a function of the Br concentration. Squares represent the results of the calculations. The straight line connects the calculated values for binary compounds.

quantitatively, and include three groups of occupied bands (a total of nine bands), the width of which does not exceed 2.4 eV. The analysis of the atomic contributions to crystal orbitals of CuCl (CuBr) demonstrates that the lower bands is formed from the Cl $3s$ states (Br $4s$ states), the energy levels in the range from −7.1 to −4.4 eV originate from the Cl $3p$ states (Br $4p$ states), and the bands in the range from −2.4 to 0 eV are predominantly formed by the Cu $3d$ states. The contribution from the Cu $3d$ orbitals to the upper bundle of bands is approximately 70%, while the rest of ~30% are due to the contribution from the p orbitals of the anion. The pseudopotential calculations of the electronic structure of copper halides in the PAO basis are in good agreement with the previously performed calculations in the FP-LAPW approximation [8], as well as with the results of recent experimental studies using X-ray photoemission spectroscopy [25].

The electronic structure of $CuCl_{1-x}Br_x$ solid solutions almost was not discussed previously. For definiteness, we consider a mixed crystal with equal concentrations of chlorine and bromine. The results of the performed calculations demonstrate that the band spectrum of $CuCl_{0.5}Br_{0.5}$ is similar to the band spectra of CuCl and CuBr, but includes not three but five groups of valence bands located in the same energy ranges as in the case of binary materials (Fig. 2). In contrast to the initial compounds CuCl and CuBr, the lower valence band of the mixed crystal consists of two subbands separated by a gap of 0.5 eV. This feature can be explained by the absence of common bonds between anions of different types in the $CuCl_{0.5}Br_{0.5}$ crystal, which substantially decreases the possible degree of hybridization of their valence orbitals. The gap of 0.5 eV between the two lower bundles of bands is caused by the difference in the energies of $3s$ and $4s$ electrons of the Cl and Br atoms, which is equal to ~0.9 eV. Similarly, owing to the difference in the ener-
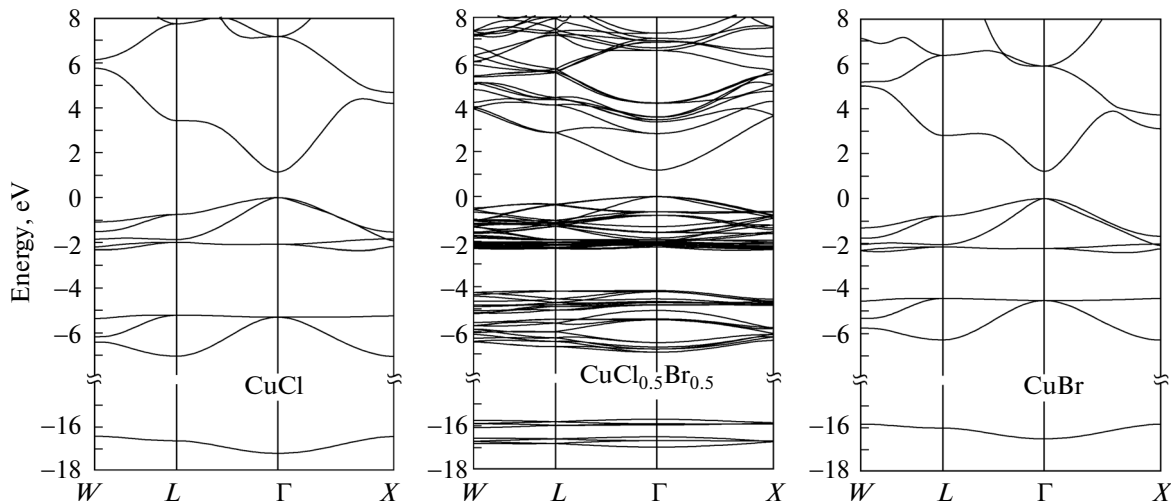
agreement with the X-ray diffraction studies [24]. The deviation of the lattice parameters from the linear dependence in our calculations does not exceed 0.06%.

Figures 2 and 3 present the results of band structure calculations for the binary compounds and the mixed $CuCl_{0.5}Br_{0.5}$ crystal, which were obtained using the exchange-correlation potentials LDA and TB09, respectively. The origin of the energy scale in all cases coincides with the top of the valence band located in the center of the Brillouin zone.

We begin the discussion with the LDA calculations. As seen from Fig. 2, the band structures of CuCl and CuBr are similar to each other, both qualitatively and

Fig. 2. Band structure of CuCl, $CuCl_{0.5}Br_{0.5}$, and CuBr according to the LDA calculations.

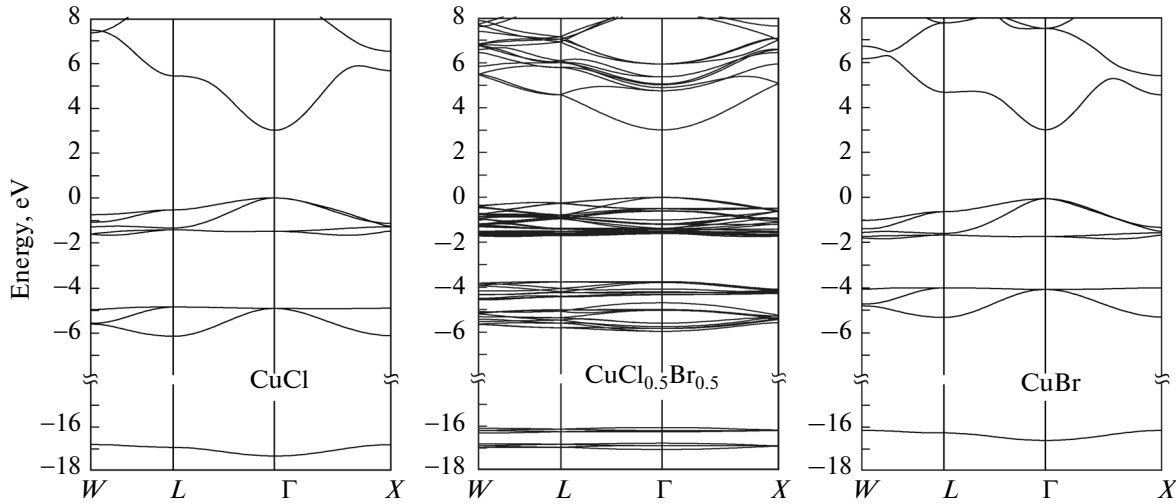**Fig. 3.** Band structure of CuCl, CuCl$_{0.5}$Br$_{0.5}$, and CuBr, calculated with the TB09 potential.

gies of Cl and Br p electrons, the contributions from the anionic p states in the range from -7 to -4 eV are unevenly distributed: in the lower half of the range, the dominant contribution comes from the Cl $3p$ orbitals, whereas the Br $4p$ orbitals play a significant role in the states located above -5.3 eV. A comparison of this picture with the contributions from the Cu $3d$ orbitals shows that the "center of gravity" of the distribution of the latter is also shifted to the region of $-(5.3-4.0)$ eV of the band under consideration. Therefore, the degree of $p-d$ hybridization of copper and bromide is higher, which can be associated with a more diffuse character of the Br $4p$ orbitals as compared to the Cl p orbitals.

The performed analysis of the nature of crystal orbitals remains valid for the results of calculations at

Energies of interband transitions in CuCl and CuBr crystals (eV)

Calculation method	$\Gamma_v - \Gamma_c$	$\Gamma_v - L_c$	$\Gamma_v - X_c$
CuCl			
TB09	3.01	5.43	5.67
LDA	1.14	3.43	4.19
GGA [8]	0.51	2.85	3.47
GGA [9]	0.54	2.85	3.40
Experiment [22]	3.40	8.1	7.8
CuBr			
TB09	3.06	4.73	4.62
LDA	1.21	2.80	3.11
GGA [8]	0.42	2.42	3.16
GGA [9]	0.39	2.4	3.1
Experiment [22]	3.07		

the TB09 level (Fig. 3). However, in this case, there is a modification of the band structure. As can be seen from the comparison of Figs. 2 and 3, the use of the exchange potential (1) leads to a contraction of the valence bands with a simultaneous shift of their upper boundaries within 0.4 eV downward (the anionic s states) or upward (middle bands) on the energy scale. It should be noted that the effect of band contraction is a characteristic feature of the TB09 application [17] and is associated with a higher degree of localization of electrons in the calculation using the Becke–Johnson potential.

Of greatest interest is the comparison of the interband transitions from the top of the valence band to the lower levels of the conduction band, which were calculated using different approximations. The table presents the energies of the transitions $\Gamma_v-\Gamma_c$, Γ_v-L_c, and Γ_v-X_c. It can be seen that the results of the E_g calculations (transition $\Gamma_v-\Gamma_c$) for copper chloride and copper bromide with the use of the same methods are close to each other. This closeness is associated with the specific features of the structure of the valence band top and the conduction band bottom of CuCl and CuBr, which have the dominant contributions from the Cu $3d$ and Cu $4s$ states, respectively. Since the anionic p bands are located energetically lower than the metal d bands, the replacement of the anion in the series of I–VII copper-containing compounds does not lead to such a large change in the band gap, which is observed in III–V semiconductors.

Our calculations within the LDA predict E_g of the considered crystals at the level of 1.1–1.2 eV. Thus, the values of E_g obtained in the LDA calculations are underestimated by 61–66% as compared to the experiment. Nonetheless, even these values are significantly higher than the results of the corresponding calculations performed in earlier studies [8, 9]. The observed

deviations are associated with the differences in details of the computational procedures and, more importantly, with the use of the localized PAO basis, which often leads to higher values of E_g as compared to the plane-wave basis. The calculations of the band structures with the TB09 potential demonstrate a significant increase in the energies of unoccupied states with respect to the upper occupied levels (compare Figs. 2 and 3). In general, we can conclude that there is a nearly uniform shift without changing the general character of the dispersion dependence of the energy branches of the conduction band. As a result of this shift, the theoretical value of E_g for the CuBr compound becomes approximately equal to the experimental value of 3.07 eV (at $T = 1.6$ K [22]), and the difference between the calculated (3.01 eV) and measured (3.40 eV at $T = 2$ K [22]) values of E_g for CuCl decreases to 0.4 eV. An increase in the value of E_g for copper halides as a result of the calculations with the TB09 potential was also demonstrated in recent studies [16, 26]. However, despite the use of the same calculation method (FP-LAPW) and program code, the results presented in [16, 26] differ significantly. Indeed, in [16], it was found that E_g is equal to 2.0 eV for CuCl and 1.8 eV for CuBr. These values are 1.7 times less than the corresponding band gaps of 3.4 and 3.0 eV, which are reported in [26]. It should be noted that the determination of the lattice constants and bulk moduli within the calculation scheme with the TB09 potential in [26] is doubtful due to the impossibility of performing the variationally consistent calculation of these characteristics, because there is no expression for exchange-correlation energy of the TB09 type. For this reason, the data presented in [16] should be considered to be more valid for the FP-LAPW method.

Figure 4 shows the composition dependences of the energies of the interband transitions $\Gamma_v-\Gamma_c$, Γ_v-L_c, and Γ_v-X_c of the mixed $CuCl_{1-x}Br_x$ crystal according to the calculations with the TB09 potential. Upon changing over to the supercell, the branches of the energy spectrum are folded due to a multiple decrease of the Brillouin zone volume. This is taken into account in Fig. 4, which presents the indirect transitions Γ_v-L_c, and Γ_v-X_c of the solid solutions for the Brillouin zone of sphalerite. Based on the presented data, we can conclude that above dependences have a nearly monotonic character, which is disturbed only for the transition Γ_v-L_c at high bromine concentrations. The change in E_g with variations in the composition of the solid solution can be described by the expression

$$E_g(x) = xE_g^{CuBr} + (1-x)E_g^{CuCl} - bx(1-x), \quad (3)$$

where b is the bowing coefficient, which determines the degree of deviation of the dependence $E_g(x)$ from the linear law. According to our calculations, the curve
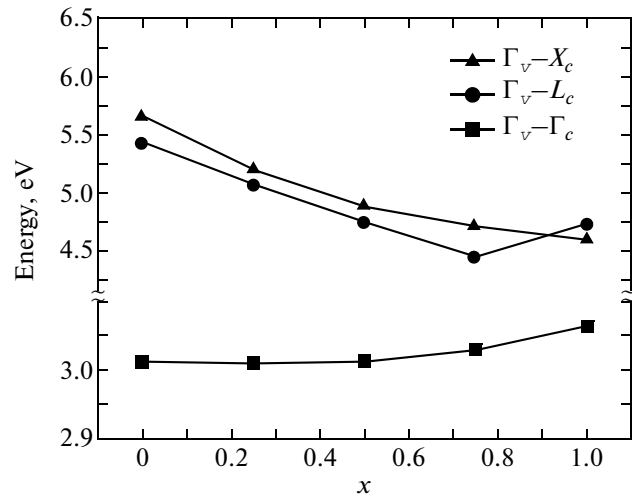

Fig. 4. Dependences of the energy of interband transitions in $CuCl_{1-x}Br_x$ on the Br concentration, calculated with the TB09 potential.

$E_g(x)$ has a small downward bowing and the parameter b is equal to 0.094 eV, which agrees with the experimental data on the exciton absorption [27]. A comparison of the results of calculations of the coefficient b in terms of the supercell method with the previously performed VCA calculations shows a higher efficiency of the supercell method for halide solid solutions. Indeed, as follows from earlier studies, regardless of the level of accuracy of the method (the fully ab initio calculations [9] or semi-empirical tight-binding calculations [23]), the VCA approach demonstrates a qualitatively incorrect dependence $E_g(x)$ for $CuCl_{1-x}Br_x$ (upward deflection) and also leads to an overestimated value of $|b|$. As was shown in [23], this effect can be eliminated by the introduction of specific corrections to the tight-binding Hamiltonian. However this approach plays a purely descriptive role, because the determination of correction requires knowledge of the composition dependence $E_g(x)$.

4. CONCLUSIONS

The electronic properties of CuCl, CuBr and mixed $CuCl_{1-x}Br_x$ crystals were investigated using the supercell method and the meta-GGA approximation. A comparative analysis of the electronic spectra revealed the similarity of the band structures of CuCl and CuBr, in which the valence band includes three bands of states spaced apart from 2 and 10 eV. The lower band is formed either by the Cl $3s$ states or by the Br $4s$ states, whereas the anionic p orbitals and the Cu d orbitals contribute mainly to the middle and upper bundles of bands, respectively. This structure of the valence band is also observed in mixed $CuCl_{1-x}Br_x$ crystals. However, owing to the difference in the energies of the s and p orbitals of the Cl and Br atoms, the

lower band of states in $CuCl_{1-x}Br_x$ is split into two closely spaced parts, and the contributions from the *p* orbitals of two types of anions in the energy range of the middle band are unevenly distributed.

It was found that the TB09 potential proposed by Tran and Blaha makes it possible to obtain the interband transition energies and band gaps of copper halides in a better agreement with experiment than in the case of the conventional LDA and GGA functionals. It was shown that the supercell method, even when using relatively small cells, is an effective tool for simulating the properties of the $CuCl_{1-x}Br_x$ solid solution.

ACKNOWLEDGMENTS

REFERENCES

1. M. Grundmann, F.-L. Schein, M. Lorenz, T. Bontgen, J. Lenzner, and H. von Wenckstern, Phys. Status Solidi A **210**, 1671 (2013).

2. D. Ahn and S. L. Chuang, Appl. Phys. Lett. **102**, 121114 (2013).

3. A. A. Eliseev, L. V. Yashina, N. I. Verbitskiy, M. M. Brzhezinskaya, M. V. Kharlamova, M. V. Chernysheva, A. V. Lukashin, N. A. Kiselev, A. S. Kumskov, B. Freitag, A. V. Generalov, A. S. Vinogradov, Y. V. Zubavichus, E. Kleimenov, and M. Nachtegaal, Carbon **50**, 4021 (2012).

4. F. O. Lucas, A. Mitra, P. J. McNally, S. Daniels, A. L. Bradley, D. M. Taylor, Y. Y. Proskuryakov, K. Durose, and D. C. Cameron, J. Phys. D: Appl. Phys. **40**, 3461 (2007).

5. K. V. Rajani, S. Daniels, M. Rahman, A. Cowley, and P. J. McNally, Mater. Lett. **111**, 63 (2013).

6. M. Ferhat, B. Bouhafs, H. Aourag, A. Zaoui, and M. Certier, Comput. Mater. Sci. **20**, 267 (2001).

7. F. El Haj Hassan, A. Zaoui, and W. Sekkal, Mater. Sci. Eng., B **87**, 40 (2001).

8. B. Amrani, T. Benmessabih, M. Tahiri, I. Chiboub, S. Hiadsi, and F. Hamdache, Physica B **381**, 179 (2006).

9. B. Ghebouli, M. A. Ghebouli, M. Fatmi, T. Chihi, Z. Heiba, and S. Boucetta, Chin. J. Phys. **51**, 738 (2013).

10. F. El Haj Hassan and A. Zaoui, Superlattice Microstruct. **30**, 75 (2001).

11. J. P. Perdew, A. Ruzsinszky, J. Tao, V. N. Staroverov, G. E. Scuseria, and G. I. Csonka, J. Chem. Phys. **123**, 062201 (2005).

12. Y. Zhao and D. G. Truhlar, J. Chem. Phys. **125**, 194101 (2006).

13. F. Tran and P. Blaha, Phys. Rev. Lett. **102**, 226401 (2009).

14. A. D. Becke and E. R. Johnson, J. Chem. Phys. **124**, 221101 (2006).

15. A. D. Becke and M. R. Roussel, Phys. Rev. A: At., Mol., Opt. Phys. **39**, 3761 (1989).

16. J. A. Camargo-Martinez and R. Baquero, Phys. Rev. B: Condens. Matter **86**, 195106 (2012).

17. A. V. Kosobutsky and Yu. M. Basalaev, Solid State Commun. **199**, 17 (2014).

18. C. Hartwigsen, S. Goedecker, and J. Hutter, Phys. Rev. B: Condens. Matter **58**, 3641 (1998).

19. A. B. Gordienko and A. S. Poplavnoi, Phys. Status Solidi B **202**, 941 (1997).

20. Yu. M. Basalaev, A. B. Gordienko, and S. I. Filippov, Phys. Solid State **54**, 1655 (2012).

21. P. Giannozzi, S. Baroni, N. Bonini, M. Calandra, R. Car, C. Cavazzoni, D. Ceresoli, G. L. Chiarotti, M. Cococcioni, I. Dabo, A. Dal Corso, S. Fabris, G. Fratesi, S. de Gironcoli, R. Gebauer, et al., J. Phys.: Condens. Matter **21**, 395502 (2009).

22. O. Madelung, *Semiconductors: Data Handbook*, 3rd ed. (Springer-Verlag, Berlin, 2004).

23. H. Heireche, B. Bouhafs, H. Aourag, M. Ferhat, and M. Certier, J. Phys. Chem. Solids **59**, 997 (1998).

24. K. Endo, K. Yamamoto, and K. Deguchi, J. Phys. Chem. Solids **54**, 357 (1993).

25. A. V. Generalov and A. S. Vinogradov, Phys. Solid State **55** (6), 1136 (2013).

26. H. Ullah, A. H. Reshak, K. Inayat, R. Ali, G. Murtaza, S. Sheraz, S. A. Khan, H. U. Din, and Z. A. Alahmed, J. Optoelectron. Adv. Mater. **16**, 1493 (2014).

27. M. Cardona, Phys. Rev. **129**, 69 (1963).

Translated by O. Borovik-Romanova